

Structures and reactions of missing dimers in epitaxial growth of Ge on Si(100)

Byung Deok Yu* and Atsushi Oshiyama

Fundamental Research Laboratories, NEC Corporation, Miyukigaoka, Tsukuba 305, Japan

(Received 13 February 1995; revised manuscript received 20 April 1995)

We present first-principles total-energy calculations for surface atomic structures which provide a natural explanation for island formation in heteroepitaxial growth of Ge on Si(100) surfaces. We first investigate structures of dimer vacancies of missing dimers (MD's) which appear on Ge overlayers on Si(100) due to lattice mismatch ($\sim 4.3\%$) between the two materials. It is found that rebonded MD's aligned straight in the direction perpendicular to dimer rows (MD lines) are stable against their meandering. This result is consistent with the recent scanning tunneling microscopy measurements and the subsequent statistical analysis. Next we investigate diffusion of a Ge atom adsorbed on the Ge overlayers which exhibit the straight MD lines. The energy barrier for diffusion along the direction of the dimer rows, along which the fast diffusion of Ge adatoms on the clean Si(100) surfaces occurs, increases by 0.8 eV near the rebonded MD. This value is much larger than the corresponding value of 0.36 eV from the previous empirical potential calculations. More importantly, this additional energy barrier is large enough to confine the Ge adatom in the flat region (on terrace) surrounded by the MD lines and thereby enhances the island formation of Ge atoms on the Ge overlayers on Si(100).

I. INTRODUCTION

Heteroepitaxial growth of semiconductors has been a challenge in both science and technology: Tailoring energy bands with the use of heterostructures is an attractive proposal in technology, and hybridizing different materials is in itself exciting in science. Significant efforts have been made for many years to achieve the growth conditions leading to high-quality films. In general, three different growth modes have been observed, depending on the nature of lattice strain and surface free energy between the overlayer material and the substrate: layer-by-layer growth (Frank-van der Merwe), multilayer islanding (Volmer-Weber), and layer-by-layer growth followed by multilayer islanding (Stranski-Krastanov). Growth of Ge films on Si(100) surfaces serves as a model system for the last case: Ge that is lower in surface energy than Si grows layer-by-layer up to several monolayers, followed by islanding due to lattice mismatch ($\sim 4.3\%$) of the two materials. In addition, several recent experiments on the heteroepitaxial growth of Ge on Si showed a variety of interesting phenomena, which include the formation of "microhuts"¹ and their coalescence leading to V-shape defects.² Microscopic atomic processes such as adatom adsorption and diffusion, which are essential in those phenomena, have not been clarified yet.

Recently Roland and Gilmer³ investigated the initial stages of the island formation on the Ge overlayers on Si(100) surfaces, using the empirical potential method. At less Ge coverage than several monolayers, the simple dimerized 2×1 structure of the Ge overlayers transforms into a $2 \times n$ ($n \approx 6 - 12$) structure in which one of the n dimers on a dimer row is missing.⁴⁻⁷ To study the diffusion process for the island formation, Roland and Gilmer calculated the potential energy surfaces seen by the Ge adatom on the film with the $2 \times n$ reconstruction. They found that the diffusion barrier along the direction

of the dimer rows increases by ~ 0.36 eV near the missing dimers (MD's). The binding site in the channel above the MD is found to be more stable by ~ 0.3 eV than the stable site on the flat region (terrace) away from the MD. Based on the low additional energy barrier near the MD and stable binding site over the MD, they argued that the channel above the MD's acts as a nucleation site for adatoms. But the three-dimensional island formation near the channel is not clearly seen in their molecular dynamics simulations for the Ge overlayers.

In this paper, we present first-principles total-energy calculations within the local-density approximation (LDA) for the island formation on the $2 \times n$ reconstructed Ge overlayer on Si(100). We first investigate structures of the MD's on the Ge overlayer. It is found that rebonded MD's aligned straight in the direction perpendicular to the dimer rows are stable against their meandering. The MD orderings thereby make the appearance of the domain separated by the MD lines possible. We further calculate pathways and energy barriers for Ge diffusion on the $2 \times n$ surface. It is found that a Ge adatom diffusing along the dimer row encounters a diffusion barrier increase of 0.8 eV near the MD's. Contrary to the previous empirical potential calculations,³ this additional energy barrier is large enough to confine the Ge adatom in the flat region (on the terrace) surrounded by the MD lines and thereby enhances the formation of atomic clusters on the terrace.

The present paper is organized as follows. In Sec. II, the calculational method is described. The results and discussion are presented in Sec. III, and concluding remarks are given in the last section.

II. METHOD

The calculations described below are based on the density functional theory⁸ using the LDA for the exchange

correlation energy.⁹ The electron-ion interaction is described by norm-conserving pseudopotentials,¹⁰ and the wave functions and thus charge densities are expanded in a plane-wave basis set.¹¹ The surface is simulated by a repeating slab model.

The ionic pseudopotentials are generated to reproduce the Si and Ge atomic spectra, following the scheme proposed by Hamann, Schlüter, and Chiang.¹⁰ The nonlocal part of the pseudopotential with the d pseudopotential as the local component is further transformed into a separable form by using a procedure suggested by Kleinman and Bylander¹² (KB). Substantial savings in computing time and storage during the iterative minimization of the total energy can be achieved using this separable nonlocal expression. This procedure is valid for the Si atom but the separable KB pseudopotential does not work for some atoms, including the Ge atom, since the logarithmic derivative of pseudo-wave-function is occasionally deviated from the all electron calculation resulting in a spurious bound state (*ghost state*).¹³ We use the real-space-partitioned pseudopotential introduced by Saito *et al.*¹⁴ to avoid the ghost states: In the method, the nonlocal pseudopotential is partitioned into two parts in the real space and then the KB procedure is applied to each part of the partitioned potential; in this procedure the ghost state is avoided by adjusting a partitioning point of the pseudopotential in the real space. For the s nonlocal potential of a Ge atom, we take $\beta = 5.0$ a.u.⁻¹ and $\alpha = 1.0$ a.u. in the expression of Eq. (9) in Ref. 14. The real-space-partitioned pseudopotential for a Ge atom is free from the ghost state and reproduces the atomic and electronic structures of the Ge crystal obtained by not using the KB procedure.

In order to perform plane-wave pseudopotential calculations on large systems, the first-principles molecular dynamics approach established by Car and Parrinello¹⁵ may be used. One of the features of the approach is that self-consistent solutions to the Kohn-Sham Hamiltonian are obtained by direct minimization of the Kohn-Sham total-energy functional. The minimization process can be accomplished either introducing fictitious dynamics to evolve the wave functions to the ground state, or by use of the steepest-descent or conjugate-gradient (CG) methods. In our calculations, we use the preconditioned CG minimization technique proposed by Bylander, Kleinman, and Lee,¹⁶ superior to other iterative minimization approaches, in which double iterative routines are employed to improve the trial wave functions and the crystal potential for a configuration of the nuclei. When this functional is minimized with respect to the wave functions, one recovers the Born-Oppenheimer energy surface, to be used in simulations of the physical trajectories of the nuclei. We optimize the geometry structure of the nuclei, using the Hellmann-Feynman forces and the efficient CG method as reported elsewhere.¹⁷

Using this formalism, we calculate the total energy and optimized atomic structure of an adatom on a crystal surface. Since the $2 \times n$ reconstruction accompanied with the MD's has been experimentally observed at a few monolayers of Ge atoms on Si(100), we here consider a three-layer Ge film labeled as $\text{Ge}_3\text{Si}(100)$. For the calculation

of $\text{Ge}_3\text{Si}(100)$, we use a slab model in a supercell, in which three Ge and two Si layers from the top surface are taken. The dangling bonds of the Si layer at the bottom surface are saturated with H atoms to have more bulklike layers (The Si-H distance is determined by the geometry optimization performed for silane SiH_4 .) The supercell consists of five atomic layers, on H layer, and an 8.57-Å vacuum region. We adsorb the Ge adatom only on one side to describe an adatom on a crystal surface. This approach reduces the slab thickness necessary for the desired accuracy. We use a 2×4 surface cell to study the diffusion of a Ge adatom on the $2 \times n$ surface. For the calculations of interactions of MD's on neighboring dimer rows we use a 4×5 surface cell. The sampling of k points in surface Brillouin zone (SBZ) integration depends on sizes of the surface cell. In the case of the 2×4 surface cell, we use 2 k points in the SBZ. For the 4×5 cell, we use 1 k point. Plane waves up to 8 Ry in kinetic energy are included in the basis set.¹⁸ The symmetry-unrestricted geometry optimization has been performed for all atoms in the slab except for the bottom-most Si and H atoms: The Si atoms at the bottom surface are in their theoretical bulk positions.¹⁹ In the optimized geometries, the remaining forces acting on the atoms are less than 0.004 Ry/Å.

Most of calculations in this paper have been performed with the above set of calculational parameters. Yet the key results are confirmed by using a more extensive set of parameters. For the diffusion of a Ge adatom on the 2×4 reconstructed surface, we have investigated the results using parameters such as the 6-atomic-layer slab, the 10-Ry-cutoff energy, and the 4 k points in the SBZ. Increasing the cutoff energy from 8 Ry to 10 Ry changed the energy differences by less than 0.05 eV per atom and increasing the number of k points from 2 to 4 resulted in changes of less than 0.02 eV per atom in the total-energy differences. Increasing the number of atomic layers from 5 to 6 (three Ge and three Si layers) changed the total-energy differences by less than 0.02 eV. From these investigations we have found that the values in the diffusion barriers of a Ge adatom presented here are accurate to 0.1 eV. For the calculations of interactions of MD's, we have also investigated the results using parameters such as the 10-Ry cutoff energy and the 2 k points in the SBZ. The 8-Ry cutoff energy and 1 k point are found to be sufficient to obtain well converged results to a numerical accuracy better than 12 meV.

III. RESULTS AND DISCUSSION

A. Structures of missing dimer

We set out the atomic structures and energetics of the clean $\text{Ge}_3\text{Si}(100)$ surface on which the $2 \times n$ reconstructions accompanied with the MD's take place. As in Si(100), Ge atoms at the surface of the $\text{Ge}_3\text{Si}(100)$ form dimers to reduce the number of Ge dangling bonds. Our total-energy calculations show that the 2×1 asymmetric dimer structure is lower in energy than the symmetric dimer structure by 0.20 eV per dimer. Alternation of

the asymmetric dimer along the dimer row corresponding to $p(2 \times 2)$ periodicity further induces the energy gain of 0.11 eV per dimer. The dimer bond length and the amount of the dimer buckling are 2.44 Å and 0.82 Å in the alternating asymmetric dimer geometry, respectively. The tilting of the dimers is 19° . The above results for the $\text{Ge}_3\text{Si}(100)$ without MD's are similar to those for the strain-free $\text{Ge}(100)$ surface.²⁰ For the latter, the 2×1 asymmetric dimer structure is lower in energy than the symmetric dimer structure by 0.24 eV per dimer; alternation of the asymmetric dimers corresponding to $c(4 \times 2)$ periodicity further induces the energy gain of 0.05 eV per dimer; the tilting of the dimers is 14° .

The $2 \times n$ reconstructed surface of the MD's are formed by removing one Ge dimer in every n dimers at the surface. The flat region between the MD's consists of alternating asymmetric dimers along the dimer row corresponding to $p(2 \times 2)$ periodicity.²¹ Here we consider the 2×4 surface, expecting that this 2×4 MD structure reasonably simulates the observed $2 \times n$ structure. Figure 1 shows the total-energy optimized atomic structure of the 2×4 MD structure. It is found that the rebonded MD structure has lower energy than the clean surface without MD's. The calculated formation energy per unit area for the rebonded MD is $-29 \text{ meV}/a_0^2$ (Ref. 22) in which $a_0 \approx 3.84 \text{ Å}$ is a surface lattice constant for $\text{Si}(100)$. The formation energy here is relative to that of the $\text{Ge}_3\text{Si}(100)$ surface with an alternation of asymmetric dimers. The negative formation energy indicates that it is energetically favorable to create the rebonded MD's in the strained Ge layers on $\text{Si}(100)$. The negative formation energy has been also obtained using the empirical potential.⁵ Removing a dimer eliminates two dangling bonds inherent to the dimer, but at the same time causes a dangling bond at each of four second-layer atoms. In the rebonded MD structure, the four Ge atoms at the second layer are rebonded, eliminate the four dangling bonds, and thereby gains the electronic energy in spite of the induced bond-length strains: The bond length between the adjacent rebonded atoms is elongated by

13–18% compared to the bulk Ge bond length. In addition, in the optimized structure, the top- and second-layer atoms near the MD are pulled towards the rebonded atoms below the dimer vacancy. Some enhanced π bonding between the dimer atoms near the rebonded MD was suggested by Pandey.²³ This is not clearly seen in our calculations on the alternating dimer structure. The atomic configuration near the rebonded MD shows a complex balance between the enhanced π bonding and the stress relief. In this paper systematic analysis of the $2 \times n$ reconstructions by varying the periodicity n are not pursued as in the empirical potential calculations.⁵ This is beyond the scope of our present work.

B. Ordering of missing dimers

An interesting feature in the MD's is their ordering in the direction perpendicular to the dimer rows: The MD's on the different dimer rows are aligned. Microscopic origin of this ordering is unresolved yet. We thus carry out total-energy calculations for the interaction between MD's. In the calculations we use a 4×5 lateral unit cell, which contains two missing dimers. With this cell, the flat region between the MD's are assumed to have the $c(4 \times 2)$ reconstruction.²⁴ Figure 2(a) shows the total-energy optimized atomic structure of the MD's without meandering. To obtain the interaction energy of the MD's on the adjacent dimer rows, we move adjacent MD by la_0 , and relax all atoms. Figures 2(b) and 2(c) show the total-energy optimized atomic structures with the one and two, respectively, lattice-constant separations ($l = 1, 2$).²⁵ It is found that the zero separation between the MD's on the neighboring dimer rows has the lowest energy. When the separation is one lattice constant, the energy becomes 68 meV higher compared to the zero separation. This value is close to the value $\sim 90 \text{ meV}$ estimated from the recent scanning tunneling microscopy (STM) experiment.⁶ We have also optimized the MD structure in which the separation of the two MD's is $2a_0$. The calculated total energy becomes 43 meV higher compared to the separation of a_0 . In our calculations, the separation of the two MD's is limited to $2a_0$ due to the small size of the unit cell. In spite of such a limitation, the interaction energies presented here qualitatively agree with the corresponding values from the STM measurements.⁶ The interaction energies monotonically increase as a function of l and, furthermore, the variation is convex in Fig. 4 in Ref. 6. The present LDA calculations clearly show that an attractive interaction exists between the MD's on the adjacent dimer rows and that the rebonded MD's aligned straight in the direction perpendicular to the dimer rows are stable. More importantly, this attractive interaction explains the appearance of the domain of the width na_0 ($n \approx 6 - 12$) separated by the MD lines.

The physical origin of the attractive interaction is the local strain around the two neighboring MD's. When the separation of the MD's on the adjacent dimer rows is one lattice constant, four additional steps in our 4×5 lateral cell are formed. In contrast with the extended

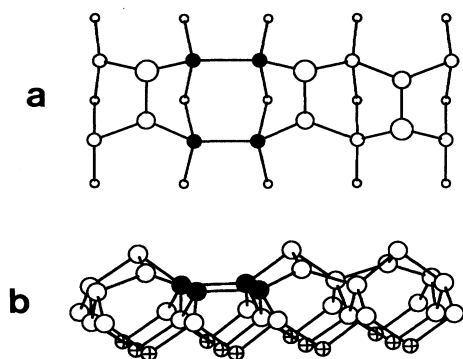


FIG. 1. Top and side views of total-energy optimized atomic structure of the rebonded missing dimer in the $\text{Ge}_3\text{Si}(100)$ of the 2×4 reconstruction. Open and crossed spheres denote Ge and Si atoms, respectively. Rebonded Ge atoms are marked by solid spheres. Atoms at lower three (a) and two (b) layers in the slab model are not shown.

steps on Si(100), the steps consist of the units with the width a_0 , which are regarded as the S_A steps²⁶ with the narrowest width. We speculate that such a geometrical structure of the S_A steps gives rise to a local strain along both parallel and perpendicular directions to the dimer rows. Therefore, the obtained energy increase of 68 meV may be interpreted intuitively in terms of the increasing number of the step units. When the separation increases from one to two lattice constants, in addition to the four S_A narrow steps, Ge atoms between the MD's undergo additional lateral strain field due to the rebonded MD's: The lateral strains can be seen in Fig. 2(c). The change in strain field along the direction perpendicular to the dimer rows is probably small. The energy increase of 43 meV for the separation $2a_0$ may be explained by the increase of lateral strain field on the system. The present total-energy calculations show that the microscopic origin for

the MD ordering in the direction perpendicular to the dimer rows is the local strain field associated with the displacement of the neighboring MD's.

C. Reactivities of missing-dimer lines

We now investigate atomic diffusion on the $2 \times n$ reconstructed MD surface. On clean Si(100) surfaces, Ge adatoms show strongly anisotropic diffusion, about 1000:1 at a typical growth temperature with the fast diffusion along dimer rows.²⁷ We expect that this fast diffusion on the surface is significantly affected by the presence of the MD's. Our study of atomic diffusion on the $2 \times n$ MD surface is concentrated on diffusion along the direction of the dimer rows. In the calculations, we use the 2×4 reconstructed surface. The optimized rebonded MD structure of alternating asymmetric dimers (Fig. 1) is used as the starting geometry on which a Ge adatom is adsorbed. The energy variations along the diffusion pathway of the Ge adatom are obtained by calculating the total energy as a function of the distance x of the adatom from the center of the MD (Fig. 3). [The dimer rows on the $\text{Ge}_3\text{Si}(100)$ surface are parallel to the x axis, and the direction of the dimer bond is along the y axis.] At each x position, we relax all atomic coordinates including y and z (vertical direction to the surface) coordinates of the adatom, and repeat the calculations for several values of the position x . We have performed the

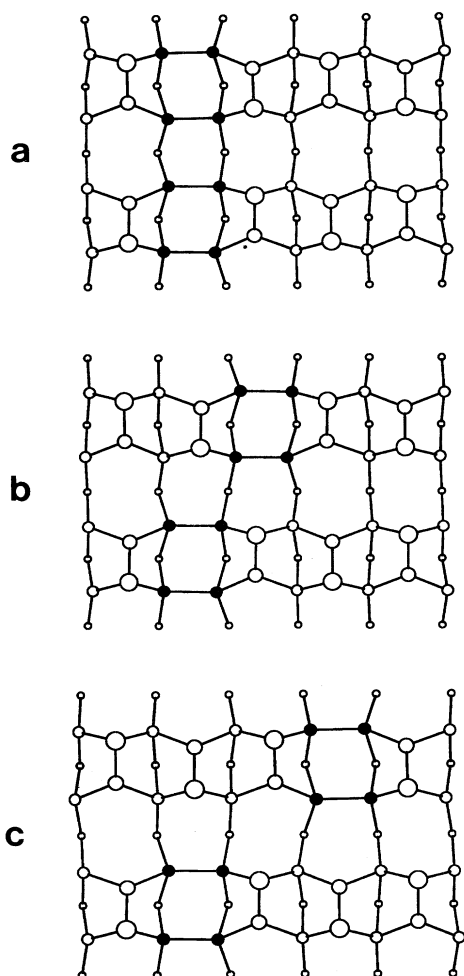


FIG. 2. Top views of total-energy optimized atomic structure of the rebonded missing dimers on the $\text{Ge}_3\text{Si}(100)$. Rebonded Ge atoms are marked by solid spheres. The separation l between the two missing dimers on the neighboring dimer rows is (a) $l = 0$, (b) $l = 1$, and (c) $l = 2$ in unit of a surface lattice constant a_0 . Each figure depicts the 4×5 periodic unit cell, which is used in the calculations.

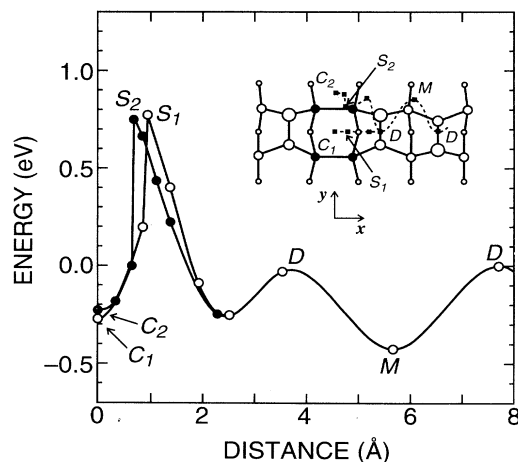


FIG. 3. Calculated total-energy variation along two reaction pathways for a Ge adatom diffusing on the 2×4 reconstructed rebonded-MD surface. In the inset, the top view of the total-energy optimized atomic structure of the rebonded missing dimer is shown. The inset also shows the pathways: Pathway B runs through the sites D, M, and D away from the MD, and then runs off the dimer row to the sites S_2 and C_2 , whereas the pathway O runs through DMD, and then runs straight to the sites S_1 and C_1 . The calculated total energies along the pathway B and along the pathway O are shown by solid and open circles, respectively. Solid squares denote some important points of the total-energy variations along the reaction pathways.

geometry optimization from a few different initial positions of y around the saddle points to avoid being trapped in a local minimum. We find two different pathways, one between the dimer rows (B) and the other on the dimer row (O), to reach the region near the rebonded MD.

When the adatom is located away from the MD's, the binding sites for the Ge adatom are similar to that for the Si adatom on the clean Si surface: The most stable position for the adatom is located at site M above the second-layer atom (Fig. 3), and the saddle point for the diffusion along the dimer row direction is located at the dimer bridge site D (Fig. 3). The calculated activation energy for diffusion along this pathway is 0.42 eV, which is 0.18 eV smaller than the corresponding value for Si diffusion on Si(100).²⁸ In the most stable geometry, the Ge adatom at site M is bonded to each atom of the two dimers of the same dimer row, and the bond lengths are 2.47 Å and 2.58 Å. The Ge adatom is also bonded to the second-layer Ge atom to make as many covalent bonds as possible, and the bond length is 2.53 Å. We have also calculated the stable adsorption sites for the Ge adatom on the strained Ge₃Si(100) without MD's, and the obtained bond lengths of the Ge adatom with the dimer atoms and the second-layer atom are 2.48 Å and 2.52 Å, respectively. The bond lengths for the adsorptions on the 2×4 reconstruction are slightly stretched compared with the corresponding values on the strained MD-free surface. This is presumably due to the lateral strain field near the MD. In addition, the bond length of one of the rebonds at the MD site is significantly elongated from its equilibrium bond length of 2.90 Å by 0.18 Å. These lateral strain fields near the MD induce a decrease of the binding energy of the Ge adatom at site M . At site D , the Ge adatoms are bonded to the two Ge atoms of the dimer. The bond lengths are found to be 2.43 Å and 2.45 Å, respectively. These values are very close to the corresponding values of 2.43 Å in the strained Ge₃Si(100) without MD's. This implies that the binding of the Ge adatom with underlying Ge dimer atoms is rarely affected by the lateral strain field near the MD. The energy increase at site M compared with site D may be attributed to the geometric restriction (the bonds with both the first- and the second-layer atoms) at site M . This energy increase leads to a smaller activation energy of the Ge adatom on the region surrounded by the MD lines compared to Si diffusion on Si(100).²⁸ We have also calculated atomic diffusion for the 2×5 reconstruction. We have obtained the activation energy of 0.41 eV for the Ge adatom diffusion similar to the value for the 2×4 reconstruction. Using the empirical potential method Roland and Gilmer³ obtained the activation energy of 0.4 eV on both surfaces with and without the rebonded MD's. In their calculations, the most stable position for the adatom in both surfaces is located at the long-bridge site in the channel separating dimer rows in contrast with our result, and the atomic diffusion along the dimer row direction takes places in the channel. They argued that this lower activation energy is attributed to the strained structure of the Ge overlayers. Our first-principles calculations, however, show that the binding sites for the Ge adatom on the strained Ge₃Si(100) without MD's are similar to

that of the $2 \times n$ reconstructed surface with MD's. It is found that the activation energy for the diffusion along the dimer rows on the surface without MD's is 0.59 eV, which is similar to that for the Si diffusion on Si(100).²⁸ A decrease in the activation energy from 0.59 eV to 0.42 eV is the consequence that the binding energy at site M is decreased due to the lateral strain fields near the MD. This is in sharp contrast with the results from the empirical potential calculations.

When the adatom approaches the rebonded MD, a further energy barrier emerges along both diffusion pathways B and O . The total energy increases as the Ge adatom passes the top-layer Ge dimer adjacent to the MD. The saddle points are located near the second-layer Ge atoms (sites S_1 and S_2 in Fig. 3). The calculated additional activation energy is 0.8 eV for both pathways. This is much larger than the corresponding value of 0.36 eV from the recent empirical potential calculations.³ Along the pathway B , the adatom forms two bonds near the MD, one with the top-layer Ge dimer atom and the other with the second-layer rebonded atom. The adatom approaches the saddle point S_2 by stretching the bond length between the adatom and the dimer atom. During the motion, the rebonded structure at the MD is not broken. The saddle point S_2 near the second-layer Ge atom corresponds to the stable binding site M on the terrace. The adsorption at the site M is stabilized by making three bonds with two top-layer Ge atoms and one second-layer Ge atom. At the site S_2 near the MD, however, one of the two top-layer Ge atoms is missing. The adatom thus forms two bonds with one top-layer Ge atom and one second-layer Ge atom. The bond lengths at the site S_2 are 2.50 Å and 2.46 Å. This decrease in the number of bonds caused by the missing top-layer atoms at the MD is the origin of the additional energy barrier. After the saddle point, the bond between the adatom and the top-layer dimer atom is broken, and a new bond between the adatom and another second-layer atom is formed by cutting one of the rebonds at the second layer. Along the pathway O , the adatom near the top-layer dimer forms two bonds with the dimer atoms. Approaching the MD, the adatom forms two bonds: one with the down atom of the first-layer buckled dimer and the other with the second-layer atom bonded with the down atom. The adatom also forms two weak bonds with the first- and second-layer atoms at the up-atom side of the dimer. During the motion, the rebonded structure at the MD is not broken. At the saddle point S_1 , the two bond lengths are 2.47 Å and 2.56 Å, and the two weak-bond lengths are 2.82 Å and 2.91 Å. After the saddle point, the bonds between the adatom and the top-layer dimer atoms are broken, and new bonds with the second-layer atoms are formed by cutting rebonds of the MD. We find that the rebonds at the second layer are preserved at the saddle points and then they are disrupted in both pathways. The total energies of sites C_1 and C_2 at the rebonded MD are both 0.15 eV higher than that of the site M , while in the empirical calculations³ the site at the MD is more stable by 0.3 eV than the most stable long-bridge site on the terrace.

The present total-energy calculations clearly show that

the Ge adatom diffusing on the $2 \times n$ reconstructed surface encounters an additional energy barrier near the rebonded MD. More importantly, this additional energy barrier of 0.8 eV is large enough to confine the Ge adatom in the flat region surrounded by the MD lines. The physical origin of the additional activation energy barrier is the decrease of the number of bonds caused by missing top-layer atoms near the rebonded MD.¹⁹ Compared to our first-principles total-energy calculations, the empirical calculations by Roland and Gilmer³ show a much smaller additional energy barrier of 0.36 eV. The most stable binding site is located in the channel above the rebonded MD. Based on the additional energy barrier near the MD and stable binding site at the MD, Roland and Gilmer³ argued that the channel above the MD's acts as a nucleation site of Ge adatoms like a step edge. This argument is in sharp contrast with our argument based on the first-principles total-energy calculations that Ge adatoms form atomic clusters *not in the channel on top of the MD's but in the flat region between the MD lines*. Our results presented here may stimulate future experimental studies of the initial stages of the island formations on the Ge overlayers on the Si surface.

The calculated results described above lead to a picture about multilayer islanding growth of Ge atoms after critical thickness (~ 3 ML) on Si(100) surface: At an initial stage of epitaxial growth of Ge on Si(100), some dimers are missing to relax lattice strain along the dimer row;⁵ with increasing Ge coverage, the MD's on different dimer rows order along the direction perpendicular to the dimer rows (MD lines);⁶ the ordered MD's induce an increase in an activation energy of a Ge adatom near the MD; the additional energy barrier confines the Ge adatoms in the flat region surrounded by the MD lines; the Ge atoms form atomic clusters on the terrace between the MD lines; subsequently, the small atomic clusters coalesce into a large island.

Finally we compare our results with a recent experimental study of Ge diffusion on the Ge overlayers on Si(100).²⁹ In STM measurements for Ge diffusion on the Ge overlayers, the diffusion coefficient is obtained by analyzing the number density of two-dimensional islands formed during deposition. The analysis shows that both the activation energy and the prefactor along the dimer rows are lower than the corresponding values for Ge (or Si) diffusion on Si(100). A value of 0.45 eV for the migration along the dimer rows was obtained, close to 0.42 eV from our first-principles calculations. Our calculations clearly show that this lower activation energy is attributed to the lateral strains caused by the rebonded MD. The additional energy barrier of the Ge adatom diffusing near the rebonded MD is expected to reduce the atomic migration from adjacent regions boarded by the MD lines. This leads to a low probability of the adatom encountering growth nuclei, and hereby reduces the prefactor for the island formation in accordance with the STM measurements.

IV. CONCLUSIONS

We have presented first-principles total-energy calculations, which provide a natural explanation for island

formation on the $2 \times n$ reconstructed surface of the Ge film on the Si(100) surface. First we studied the ordering of the MD's in the direction perpendicular to the dimer rows. By performing the total-energy calculations, we obtained the magnitude of the MD-MD interactions and their microscopic origins. It is found that the rebonded MD's aligned straight in the direction perpendicular to the dimer rows are stable. The present calculations clearly show an attractive nature of the two MD's on the adjacent dimer rows. The calculated interaction energies qualitatively agree with the corresponding values from the STM measurements. The physical origin of the attractive interactions is the local strain field associated with the displacement of the neighboring MD's. More importantly, the attractive interactions make the appearance of the domain separated by the MD lines likely.

Next we have studied reactivities of the MD's on the $2 \times n$ reconstructed surface to clarify the role of the MD's in heteroepitaxial growth of Ge on Si(100). Contrary to the empirical potential calculations, we have found that the most stable position for the Ge adatom is located at the site off the dimer rows in the flat region between the MD lines. The saddle point for the diffusion along the dimer row on the flat region is the site on the dimer. The calculated activation energy along this path is 0.42 eV, which is 0.18 eV smaller than the corresponding value for Si diffusion on Si(100). We have found that the lower energy barrier compared to the surface without MD's is attributed to the additional lateral strain field near the MD caused by atomic adsorption. The Ge adatom encounters an additional energy barrier near the rebonded MD. The calculated increase in the energy barrier is 0.8 eV much larger than that of the empirical potential calculations. This additional energy barrier is large enough to confine the Ge adatom in the flat region surrounded by the MD lines. The physical origin of this increase of the energy barrier is the decrease of the number of bonds caused by missing top-layer atoms near the rebonded MD. In addition to the confinement of the Ge atomic motion, the additional energy barrier prevents Ge adatoms from reaching step edges and thereby obstructs step flow for crystal growth. In epitaxial growth of the semiconductor, layer-by-layer growth typically proceeds with the step-flow mechanism. This indicates that the additional energy barrier leads to the multilayer islanding growth by confining the Ge atomic motions on the terrace between the MD lines and obstructing the step flow. The present LDA calculations provide an explanation for the microscopic mechanism of the multilayer islanding growth on the Ge overlayers on the Si(100) surface.

ACKNOWLEDGMENTS

We are grateful to T. Ide and K. Watanabe for useful discussion on the STM measurements. We wish to thank Y. Miyamoto, M. Saito, and O. Sugino for discussion on the calculational technique.

- * Present address: Fritz-Haber-Institut der Max-Planck-Gesellschaft, Faradayweg 4-6, D-14195 Berlin-Dahlem, Germany.
- ¹ Y. -W. Mo, D. E. Savage, B. S. Swartzentruber, and M. G. Lagally, Phys. Rev. Lett. **65**, 1020 (1990).
 - ² A. Sakai and T. Tatsumi, Phys. Rev. Lett. **71**, 4007 (1993).
 - ³ C. Roland and G. H. Gilmer, Phys. Rev. B **47**, 16 286 (1993).
 - ⁴ Y. -W. Mo and M. G. Lagally, J. Cryst. Growth **111**, 876 (1991); U. Köhler, O. Jusko, B. Müller, M. Horn-von Hoe-gen, and M. Pook, Ultramicroscopy **42-44**, 832 (1992); R. Butz and S. Kampers, Appl. Phys. Lett. **61**, 1307 (1992).
 - ⁵ J. Tersoff, Phys. Rev. B **45**, 8833 (1992).
 - ⁶ X. Chen, F. Wu, Z. Zhang, and M. G. Lagally, Phys. Rev. Lett. **73**, 850 (1994).
 - ⁷ The observed average distance between MD's depends on Ge coverage. Recent STM observations (Ref. 6) show that $n \sim 9$ for the Ge coverage of ~ 1.5 ML.
 - ⁸ W. Kohn and L. J. Sham, Phys. Rev. **140**, A1133 (1965).
 - ⁹ D. M. Ceperley and B. J. Alder, Phys. Rev. Lett. **45**, 566 (1980).
 - ¹⁰ D. R. Hamann, M. Schlüter, and C. Chiang, Phys. Rev. Lett. **43**, 1494 (1979).
 - ¹¹ J. Ihm, A. Zunger, and M. L. Cohen, J. Phys. C **12**, 4409 (1979).
 - ¹² L. Kleinman and D. M. Bylander, Phys. Rev. Lett. **48**, 1425 (1982).
 - ¹³ X. Gonze, P. Käckell, and M. Scheffler, Phys. Rev. B **41**, 12 264 (1990).
 - ¹⁴ M. Saito, O. Sugino, and A. Oshiyama, Phys. Rev. B **46**, 2606 (1992).
 - ¹⁵ R. Car and M. Parrinello, Phys. Rev. Lett. **55**, 2471 (1985).
 - ¹⁶ D. M. Bylander, L. Kleinman, and S. Lee, Phys. Rev. B **42**, 1394 (1990).
 - ¹⁷ O. Sugino and A. Oshiyama, Phys. Rev. Lett. **68**, 1858 (1992); B. D. Yu and A. Oshiyama, *ibid.* **71**, 585 (1993).
 - ¹⁸ The equilibrium lattice constant of Si for a basis set with a cutoff energy of 8 Ry and a k point sampling used for the surface calculations is 5.43 Å, which is very close to the experimental value. For Ge we obtain the equilibrium lattice constant of 5.61 Å, which is 0.8% smaller than the experimental value. This leads to lattice mismatch of 3.3% between the two materials. This value is 1.0% smaller than the experimental value of 4.3%.
 - ¹⁹ A. Oshiyama, Phys. Rev. Lett. **74**, 130 (1995).
 - ²⁰ M. Needels, M. C. Payne, and J. D. Joannopoulos, Phys. Rev. Lett. **58**, 1765 (1987).
 - ²¹ Recent STM measurements (Ref. 6) show that the flat region between the MD lines reconstructs into the $c(4 \times 2)$ structure. Our first-principles total-energy calculations of the $\text{Ge}_3\text{Si}(100)$ surface without MD's show that the $c(4 \times 2)$ structure has the lowest energy. Yet the $p(2 \times 2)$ reconstruction is nearly degenerate with the $c(4 \times 2)$ reconstruction: Its energy is higher by only 10 meV per dimer. We thus assume here that the $p(2 \times 2)$ structure well simulates the flat region for the $2 \times n$ surface calculations.
 - ²² This value of $-29 \text{ meV}/a_0^2$ corresponds to -232 meV per $8a_0^2$ (i.e., per unit cell). In this calculation of the formation energy of the MD, we take the value of strained bulk Ge as chemical potential of Ge atoms. When we assume the chemical potential of unstrained bulk Ge, the formation energy becomes $-35 \text{ meV}/a_0^2$. This still indicates that it is energetically favorable to create the rebonded MD's in the $\text{Ge}_3\text{Si}(100)$.
 - ²³ K. C. Pandey, in *Proceedings of the Seventeenth International Conference on the Physics of Semiconductors*, edited by J. D. Chadi and W. A. Harrison (Springer-Verlag, New York, 1985), p. 55.
 - ²⁴ By this assumption, the two asymmetric dimers on either side of the MD are buckled in the opposite direction. The total-energy comparison between this geometry with another where they are buckled in the same direction has not been performed, expecting the minor total-energy difference.
 - ²⁵ In the present unit cell, the separation l corresponds to two misalignments: l and $5 - l$.
 - ²⁶ D. J. Chadi, Phys. Rev. Lett. **59**, 1691 (1987).
 - ²⁷ Y. -W. Mo and M. G. Lagally, Surf. Sci. **248**, 313 (1991).
 - ²⁸ G. Brocks, P. J. Kelly, and R. Car, Phys. Rev. Lett. **66**, 1729 (1991); Y. W. Mo, J. Kleiner, M. B. Webb, and M. G. Lagally, *ibid.* **66**, 1998 (1991).
 - ²⁹ M. G. Lagally, Jpn. J. Appl. Phys. **32**, 1493 (1993).